Nuclear-targeted gold nanoparticles enhance cancer cell radiosensitization

To cite this article before publication: Serdar Ozcelik *et al* 2020 *Nanotechnology* in press https://doi.org/10.1088/1361-6528/aba02b

IOP Publishing Nanotechnology
Nanotechnology **25** (2020) XXXXXX https://doi.org/10.1088/XXXX

Nuclear-targeted gold nanoparticles enhance cancer cell radiosensitization

Serdar Özçelik[1, 2] and Guillem Pratx[2]

[1] İzmir Institute of Technology, Department of Chemistry, Gülbahçe-Urla, 35430 İzmir, Turkey
[2] Department of Radiation Oncology, Stanford University School of Medicine, Stanford, California 94305, USA

E-mail: serdarozcelik@iyte.edu.tr

Received xx xx 2020
Accepted for publication xxxxxx
Published xxxxxx

Abstract

Radiation therapy aims to kill or inhibit proliferation of cancer cells while sparing normal cells. To enhance radiosensitization, we developed 40 nm-sized gold nanoparticles targeting the nucleus. We exploited a strategy that combined RGD and NLS peptides respectively targeting cancer cell and the nucleus to initiate cell-death activated by X-ray irradiation. We observed that the modified gold nanoparticles were either translocated in the nuclei or accumulated in the vicinity of the nuclei. We demonstrated that X-ray irradiation at 225 kVp energy reduced cell proliferation by 3.8-fold when the nuclear targeted gold nanoparticles were used. We determined that the radiation dose to have a 10% survival fraction was reduced from 11.0 Gy to 7.1 Gy when 10.0 μg/mL of the NLS/RGD/PEG-AuNP was incubated with A549 cancer cells. We conclude that the peptide-modified gold nanoparticles targeting the nucleus significantly enhance radiosensitization.

Keywords: Gold nanoparticles, nuclear targeting, NLS peptide modification, radiosensitization

1. Introduction

Radiation therapy is one of the methods used in cancer treatment. The aim of radiation therapy is to selectively kill or reduce the proliferation of cells in tumors while minimizing damages to healthy tissue. Its success remains limited due to tumor heterogeneity and adverse effects on surrounding healthy tissues [1, 2]. The pioneering in-vivo study by Hainfeld et al. demonstrated the ability of gold nanoparticles as a potent radiosensitizers [3]. Since then, many pre-clinical investigations examined physical, chemical, and biological effects induced by gold nanoparticles [4, 5]. To make a meaningful comparison among studies is problematical because particle and radiation parameters as well as cell types are very diverse. However, there are two particular studies worth mentioning because they are related to our work presented here. Wang et al. used 20 nM of 13 nm glucose-coated gold nanoparticles and irradiated A549 cells at 6 megavoltage. They concluded that a dose enhancement of 1.49 increased apoptosis and caused cell cycle arrest at G2/M phase [6]. Another study, published as a conference abstract, used the Panc-1 human pancreatic adenocarcinoma cancer cells and irradiated them with different radiation sources including 250 keV X-ray [7]. They reported higher radiosensitization and higher DNA damage for nuclear targeted AuNP compared to pegylated AuNP and, but no further details were provided in the abstract.

The effectiveness of radiation in killing cancer cells has been shown to increase in the presence of gold nanoparticles due to physical increase in local dose deposition. Enhancement in radiotherapeutic efficiency means that lower radiation doses would be used, and therefore adverse effects of radiation therapy may be reduced provided that the nanoparticles

remain confined to tumor cells. In other words, more cancer cells would be killed by a typical radiation dose (2 Gy per fraction) used for cancer treatment [8]. But, effective radiosensitization induced by gold nanoparticles was inadequate so far for clinical translation.

Killing cancer cells effectively by gold nanoparticles may require targeting cancer cells and sub-organelles such as nuclei. This strategy may increase success of radiation therapy and minimize adverse effects on healthy cells. But, the effect of nuclear targeted gold nanoparticles combined with irradiation surprisingly has not been evaluated. The reason for targeting nucleus lies in the fact that nucleus is thought to be the primary target of radiation therapy, therefore the nanoparticles must be located near DNA to maximize the physical dose enhancement. Indeed, microdosimetry simulations have shown that the dose enhancement around gold nanoparticles decays rapidly away from the nanoparticle [10].

There are three main reasons for this rapid decay. First, due to purely geometric factors, the dose-enhancing effect of electrons emitted from gold nanoparticles falls off as inverse of the distance squared. A second effect is that irradiated gold nanoparticles release Auger electrons, which in turn may stimulate chemical and biological mechanisms to damage DNA for effective cell killing [9 – 14]. These electrons are emitted with energy ranging from 50 eV to 2000 eV. They have shorter range and are more densely ionizing (and thus lethal) than the typical secondary electrons produced during conventional irradiation [15]. Third, low-energy electrons with energy below 10 eV are tertiary particles that are non-ionizing but can nevertheless induce single and double DNA strand breaks [https://science.sciencemag.org/content/287/5458/1658].

Damage by low-energy electrons is significantly enhanced by gold nanoparticles, but only when the DNA is located in close proximity to the nanoparticles [https://www.ncbi.nlm.nih.gov/pmc/articles/PMC3829822/].

These effects together contribute to a rapid fall-off of the dose-enhancing effect of gold nanoparticles. Therefore, nanoparticles are most effective they accumulate in the vicinity of the nucleus and other radiation-sensitive organelles, such as mitochondria [16]. Hence, we hypothesized that higher cell killing could be achieved by localizing the gold nanoparticles to the nucleus.

Cell membrane regulates cellular entry of nanoparticles. There are several internalization mechanisms including phagocytosis, pinocytosis, receptor mediated endocytosis, and passive diffusions. [17 -19] There is a general consensus that small nanoparticles may pass the cell membrane passively, however, the passage of larger nanoparticles may vary with cell type, nanoparticle size, materials, and their physicochemical properties. Phagocytosis is limited to specialized cell such as macrophages while pinocytosis is more general and classified into clathrin mediated endocytosis, caveoli mediated endocytosis, clathrin and caveoli independent endocytosis, and micropinocytosis. [20]. Nanoparticles utilizing caveolae-mediated endocytosis circumvents sorting in endosomes and move through by caveosomes (a lipid droplets with a neutral pH) where contents are delivered to non-lysosomal subcellular compartments such as the endoplasmic reticulum [21]. The endoplasmic reticulum continues with the nuclear membrane, assisting nanoparticles in reaching nucleus. The popularity and success of SV40 nuclear localization sequence (NLS) is partly attributed to caveolae-mediated endocytosis [22].

Nuclear membrane separates the nuclear contents from the cytoplasm and prevents the free passage of cytoplasmic contents [23]. The nuclear membrane contains nuclear pore complexes (NPC; approximate diameter of 30 nm) that actively controls the passage of larger nanoparticles. While small nanoparticles are able to pass through the NPC by passive diffusion, larger ones must possess NLS [24]. When gold nanoparticles (40 nm diameter) and magnetite nanoparticles (50 nm diameter) are conjugated with NLS, they are taken up through the nuclear pore complexes using a carrier protein called importin [26, 27]. It has also been reported that large nanoparticles can enter the nucleus once the nuclear membrane breaks down during mitosis [28]. The break-down of the nuclear membrane might assist larger nanoparticles in entering the nucleus. But this does not exclude that modifications in transport machinery and structural changes in the nuclear membrane occur in cancer cells and facilitate entry of large nanoparticles into the nucleus.

In this study, we developed peptide-modified gold nanoparticles targeted to the nucleus by utilizing nuclear localization signal (NLS) peptides and by RGD peptides recognizing integrin receptors on cancer cell membrane. We then evaluated the radiation dose required to reduce cell proliferation and increase cell killing. We calculated a dose enhancement factor of 1.55 when A549 cells were incubated with 10 μg/mL peptide-modified gold nanoparticle. The critical factor for this enhancement is effective nuclear targeting and accumulation of the peptide-modified gold nanoparticles.

2. Materials and Methods

2.1 Materials

Hydrogen tetrachloroaurate (III) trihydrate ($HAuCl_4.3H_2O$, 99%) and trisodium citrate dehydrate were purchased from

Sigma Aldrich. Ultrapure water was obtained from a Millipore instrument for solution preparation. RGD peptide (L-arginyl-glycyl-L-aspartic acid) from Sigma- Aldrich, thiol modified methoxypolyethyelene glycol, mPEG-SH 2000 from Laysan Bio, and NLS peptide (Cys-Gly-Tyr-Gly-Pro-Lys-Lys-Lys-Arg-Lys-Val-Gly-Gly), a synthetic peptide homologous to the SV40 T antigen from Santa Cruz were purchased.

2.2 Instrumentation

Nanoparticles were characterized by optical and structural measurements. UV-Visible absorption spectra were recorded with a Varian Cary 50 UV-Vis spectrophotometer. Particle size distribution and zeta potential measurements were performed by the dynamic light scattering method using a Malvern ZETASIZER-ZS. Scanning electron microscopy for structural characterizations was performed by a field emission scanning electron microscope, FEI QUANTA 250 FEG operating at 15.0 kV. The molar concentrations of nanoparticles were determined by UV-Vis. spectroscopy and confirmed by inductively coupled plasma-mass spectrometry using an Agilent 7500ce. Cell images were taken by a spinning disc confocal microscope (Andor Revolution) equipped with differential interference contrast and dark-field attachments.

2.3 Synthesis of gold nanoparticles

A modified Turkevich method was used to synthesize gold nanoparticles with size of 40 nm. Typically, 50 mL of 0.25 mM $HAuCl_4$ solution was heated to 120 ^oC under reflux. A 0.25 mL of 1% solution (by mass) of trisodium citrate was rapidly added to this boiling solution and stirred until the color of the solution turned to red, typically it took 15 minutes. The synthesized nanoparticles were purified by centrifugation, operating at 6.000 rpm for 15 minutes and purification repeated twice.

2.4 Preparation of peptide-modified gold nanoparticles

Polyethylene glycol (PEG) conjugation prevents aggregation of gold nanoparticles and reduce cytotoxicity. The purified gold nanoparticles were re-dispersed in distilled water. A 0.2 mM stock solution of mPEG-SH 2000 was prepared in distilled water. A dispersion of 7.5 mL of 0.24 nM of gold nanoparticles was incubated with 10 mL of 0.2 mM of mPEG-SH 2000 for 24 hours at room temperature. Excess PEG was removed by centrifugation (6.000 rpm, 15 minutes) to obtain purified PEG-AuNP.

The PEG-AuNPs were conjugated with RGD peptides. 2.6 μL of 5 mM RGD in distilled water was added to 7.5 mL of 0.24 nM of PEG-AuNPs dispersion and allowed to mix for 48 hours at room temperature. The excess RGD peptides were removed by centrifugation (6.000 rpm, 15 minutes). The modified gold nanoparticles (RGD/PEG-AuNPs) would be dispersed in distilled water or in cell culture media.

To get NLS conjugated AuNPs, a solution of 1.00 mL of 0.5 mM NLS in distilled water was added to 7.5 mL of 0.24 nM of PEG-AuNPs dispersion. Centrifugation was used to purify the nanoparticles and remove unbound NLS peptides, for 15 min. at 6.000 rpm, to obtain NLS/PEG-AuNPs. We used concentrated dispersion of gold nanoparticles in the experiments.

NLS/RGD/PEG-AuNP were prepared by mixing a solution of 1.0 mL of 0.5 mM NLS in distilled water with a 7.5 mL of 0.24 nM of RGD/PEG-AuNPs dispersion for 48 hours at room temperature. The modified nanoparticles were purified by centrifugation (15 min. at 6.000 rpm, twice).

2.5 Cell culture

A549 cells (a human lung carcinoma epithelial cell line) were purchased from American Type Culture Collection and maintained in DMEM/F-12. Basal media were supplemented with %10 FBS (fetal bovine serum), %1 penicillin and %1 L-glutamine. Cell cultures were kept at 37 ^0C in a 5 % CO_2 humidified incubator. Cells were seeded in 6-well plates for irradiation.

2.6 Irradiation of cells

The prepared cells were irradiated with a Kimtron IC250 irradiator operating at 225 kV and 13 mA, providing a dose rate of 1.03 Gy/min after filtration with 0.5 mm Cu at a source-to-surface distance of 50 cm. Regular output calibration is performed twice per year by medical physics staff using a PTW Farmer ionization chamber that is cross-calibrated to a NIST-traceable ionization chamber. Dose uncertainty is estimated as ± 10%. A radiation dose of 0 - 8 Gy was used in the experiments. The distance between the source and the 6-well plate was set to 50 cm. The irradiator was configured to automatically stop when the preset dose was achieved.

2.7 Clonogenic assay and analysis

The A549 cells were grown in T-25 flask. The day before irradiation, 1000 cells per well in a six-well plate were seeded for 0 – 4 Gray radiation doses, and 2000 cells per well in a six-well plate were seeded for 8 Gray radiation doses. Two hours following the seeding, attachment of individual cells to the bottom of the wells was confirmed by an optical microscope. Then, the cells were incubated for 24 hours with various

amounts (up to 10 μg/mL) of peptide modified gold nanoparticles (RGD/PEG, NLS/PEG and RGD/NLS/PEG). Before irradiation, the cell medium was replaced with fresh medium, eliminating residual gold nanoparticles that were not internalized. After 7 days, each well was fixed and stained with a 2.5 mL mixture of 4% glutaraldehyde and % 0.5 crystal violet in water. Stained cell colonies were counted by ImageJ using a colony counting plug-in developed by Guzman et al [29]. The t-test was applied for statistical analysis of the assay results.

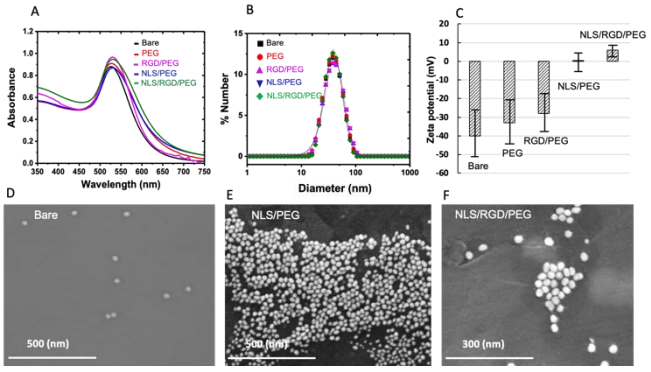

Figure 1: The physicochemical properties of gold nanoparticles. A) UV-Vis absorption spectra of bare (citrate coated), PEG-coated and peptide-modified gold nanoparticles. B) DLS size (diameter) distribution of the AuNPs without and with surface modifications. C) Zeta potentials, as mean ± standard deviation, $p < 0.001$ for NLS/PEG and NLS/RGD/PEG modifications compared to bare nanoparticles. Scanning electron microscopic images of gold nanoparticles, bare (D), NLS/PEG modified (E) and NLS/RGD/PEG modified (F).

3. Results

3.1 Properties of gold nanoparticles

Figure 1 represents spectroscopic and structural properties of gold nanoparticles modified with NLS and RGD peptides. UV-Visible spectroscopy shows characteristic plasmonic band of the gold nanoparticles with and without peptides, having spectra centered at 530 nm (Fig. 1. A). Peptide modification did not change the plasmonic spectral shape and positions of gold nanoparticles. The nanoparticles are mono-dispersed and their size distributions is centered at 40 nm. Scanning electron microscopic images (Fig. 1. D - F) showed the shape and size distribution of the nanoparticles were not affected by the peptide modification, confirming DLS measurements. Although the size and shape of the gold nanoparticles were not changed, the zeta potential increased from -33 mV to 6 mV by the peptides, verifying the peptide modification.

3.2 Cellular uptake and distribution of the peptide modified gold nanoparticles

We first assessed the number of gold nanoparticles using ICP-MS and UV-Vis. measurements. We calculated that there were 8×10^{10} nanoparticles per mL (34 μg/mL). Then we examined uptake of the peptide modified AuNPs. Using ICP-MS and UV-Vis absorbance, we determined the fractional uptake of peptide modified AuNPs after incubation with 10^5 cells/well for 24 hours (percent uptake shown in Figure 2). The amount of modified gold nanoparticle reached 0.24 ng per cell when 70% of the peptide modified AuNP was internalized. No cytotoxicity is observed up to 25 μg/mL of AuNP concentration per well.

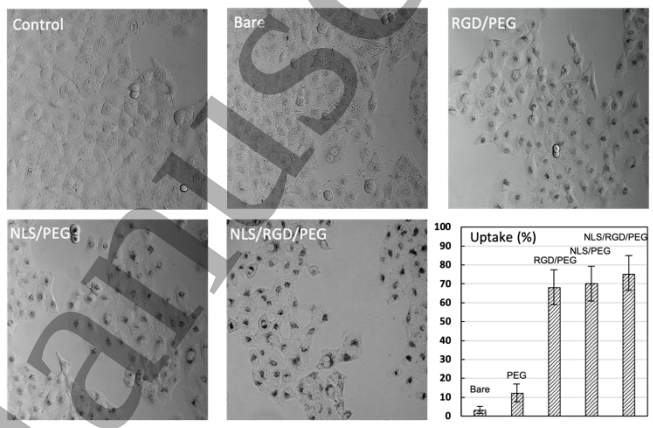

Figure 2: Cellular uptake of AuNPs. Each image is labelled with the type of gold nanoparticles incubated with the cells (20x objective, a field of view is 500 x 500 μm). The amount of AuNPs internalized are presented as mean ± standard deviation, n=3, $p < 0.001$ for peptide modified AuNPs compared to bare.

Optical microscopy was employed to monitor the distribution of the gold nanoparticles taken up by cells. Figure 2 shows brightfield images of A549 cells incubated with the gold nanoparticles modified with peptides as well as control cells. The control image (Fig.2) shows A549 cells in a healthy condition. The uptake of AuNPs as a percentage is given as a bar graph in Fig. 2. Dark spots in these images represent the location of AuNPs.

When AuNPs were modified with RGD/NLS/PEG and NLS/PEG, more nanoparticles were internalized in the cells. The peptide modified AuNPs (NLS/RGD/PEG and NLS/PEG) as shown in Figure 2 were mostly located in and around nuclei, proving that targeting nucleus with NLS peptide was effective. Darker spots were observed when NLS/RGD/PEG-AuNPs were used, meaning that more particles per dark spot. When bare AuNPs were incubated with cells, AuNPs were randomly distributed in the cytoplasm.

We furthermore used confocal microscopy to validate nuclear translocation of peptide modified AuNPs. Figure 3 shows differential interference contrast (DIC) images of cells incubated with bare, NLS/PEG and NLS/RGD/PEG modified AuNPs. The dark spots seen in the nuclei revealed the gold

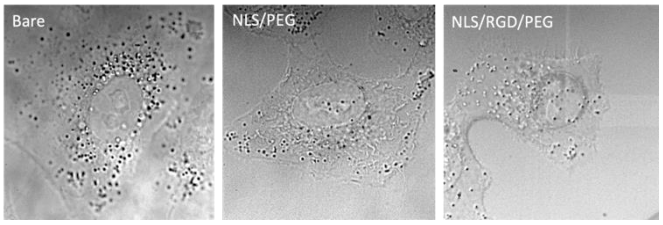

Figure 3: DIC contrast confocal microscopic images (100x objective, a field of view is 50 x 50 μm) of A549 cells treated with bare, NLS/PEG and NLS/RGD/PEG AuNPs. The dark spots inside the nuclei represent the gold nanoparticles. Bright and dark spots in the cytoplasm are gold nanoparticles and vacuoles having higher refractive index. Note that vacuoles do not appear in the nucleus for cell incubated with bare AuNPs.

nanoparticles coated with NLS peptide are translocated in nucleus. The modified nanoparticles also accumulated in proximity to the nuclear membrane. The dark spot sizes are larger than 3x3 pixels (optical resolution of the microscope), so there should be many gold nanoparticles per spot, however, the exact number is hard to estimate. We note that bright and dark spots appearing in the cytoplasm are due to AuNPs as well as vacuoles. No vacuoles are seen in the nucleus. A549 cells contains many vacuoles and they are easily observable by DIC contrast because of higher refractive index compared to water-based cytoplasmic medium as seen in Fig.3.

3.3 Clonogenic Assay

Clonogenic assay experiments were performed to assess cell survival fractions after X-ray irradiation treatment of cells. The cells were incubated with the modified gold nanoparticles with various peptide combinations: RGD/PEG, NLS/PEG and NLS/RGD/PEG. Figure 4 illustrates how peptide modification alters the cell survival fractions. The survival fractions (SF) were examined by varying the irradiation doses. At 4 Gy, the RGD modification slightly reduced the survival fraction. The survival fraction decreased by 20% and 25% for NLS and NLS/RGD modifications, respectively, compared to irradiated control without nanoparticle. A 3.8-fold reduction in the survival fraction at 8 Gy was observed for the NLS/RGD modification compared to irradiated controls. The NLS-only modification was also effective, reducing survival more than 3-fold. As a result, the nuclear targeting by modifying the gold nanoparticles with NLS and RGD peptides is effective to increase cell killing upon X-ray irradiation.

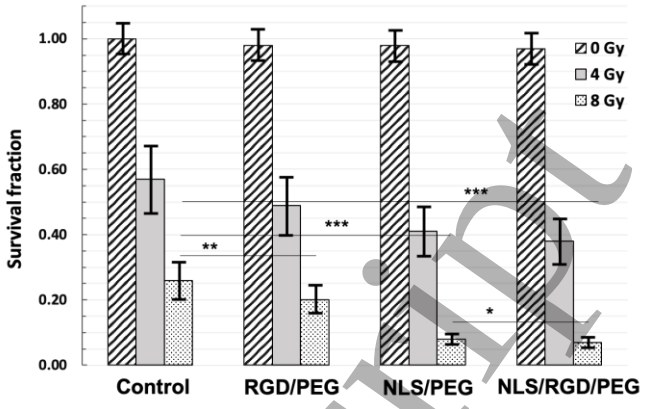

Figure 4: The survival fractions as a function of peptide modifications. PEG is omitted in the labelling for simplification. The radiation doses are provided. Data are shown as mean ± standard deviation; n = 3, * $p > 0.05$, ** $p < 0.05$, *** $p < 0.001$, and all others $p > 0.05$.

Figure 5 demonstrates a dose-dependent effect of RGD/NLS/PEG modified AuNPs on the survival fraction. We varied the amount of AuNPs from 1.0 to 10.0 μg/mL. We determined that the radiation dose to have a 10% survival fraction was significantly reduced from 11.0 Gy to 7.1 Gy when 10.0 μg/mL of the NLS/RGD/PEG modified gold nanoparticles was used. The radiation enhancement factor is accordingly 1.55 for the 225 kVp irradiation energy. This enhancement may be gained because the gold nanoparticles modified with NLS/RGD/PEG are closer to nuclei.

The survival data were also analysed according to the linear-quadratic model in which the survival fraction (SF) was estimated using the equation: $SF = \exp(-\alpha D - \beta D^2)$, where D is the irradiation dose. We used non-linear regression to obtain α and β values. Table 1 summarizes the radiation enhancement factors depending on the amount of the modified gold nanoparticles, and α, β and R^2 values as the fitting parameters. The analysis revealed that the fitting parameters α and β increased about 2-fold with increasing nanoparticle concentration. To assess whether this increase was consistent with a pure dose enhancement effect, we computed α/DEF and β/DEF^2 (Table 1). The parameter α increased faster than the DEF, suggesting an increase in the rate of single-hit cell killing. In comparison β remained proportional to DEF^2. Therefore, the effect of the nanoparticles includes an increase in the local energy deposition, which is modelled by the DEF, and an additional increase in the rate of single-hit damage. This latter effect is likely due to the higher linear energy transfer (LET) of Auger electrons that are emitted by the gold nanoparticles.

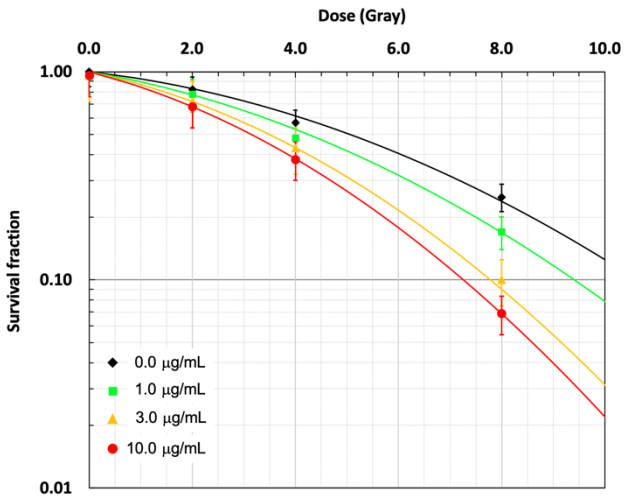

Figure 5: Cell survival fractions of A549 cell incubated with increased amount of NLS/RGD/PEG modified AuNPs. The solid curves are the fit to the linear-quadratic equation. Data are shown as mean ± standard deviation. n = 3, $p < 0.001$ for the amounts of 3.0 and 10.0 µg/mL with respect to 0.0 µg/mL at 8 Gy, all others $p > 0.05$. Table 1 summarizes the fitting parameters.

Table 1: Dose required to achieve 10% survival fraction (D_{10}), dose enhancement factor (DEF) calculated at 10% survival, , and fitting parameters α and β values for different amount of NLS/RGD/PEG-AuNP.

AuNP (∝g/mL)	D_{10} (Gy)	DEF	a (Gy^{-1})	b (Gy^{-2})	R^2	a / DEF	b / DEF^2
0.0	11.00	1.00	0.088	0.011	0.998	0.088	0.011
1.0	9.20	1.20	0.108	0.015	0.983	0.090	0.010
3.0	8.00	1.38	0.125	0.021	0.994	0.091	0.011
10.0	7.10	1.55	0.146	0.024	0.995	0.094	0.010

4. Discussion

Radiation therapy affects both cancerous and healthy cells. To enhance the efficacy of radiation therapy and reduce adverse effects, gold nanoparticles were introduced as a potential radiosensitizer [3]. In this approach, cells are treated with gold nanoparticles that enhance the local deposition of ionizing energy by irradiation, thereby destroying targeted cancer cells but sparing normal cells. Considerable evidence shows that the nucleus is the primary target for radiation therapy because it controls cell survival, growth, proliferation, and death. Since the local dose enhancement effect due to Auger and low-energy electrons is highest near the surface of the nanoparticles [9-12], delivery and accumulation of gold nanoparticles to the nucleus become critical to initiate DNA damage.

The physical enhancement of X-ray radiation depends on size and number of gold nanoparticles, their cellular location, as well as the photon energies used for irradiation. We kept the size of AuNP unchanged but varied their concentration (1.0 to 10.0 µg/mL) in the culture medium. The photon energy was constant at 225 kVp and the dose was varied from 2- 8 Gy. In this study, the modified gold nanoparticles were targeted to nucleus using NLS and RGD peptides. Integrin receptors are over-expressed in many cancer cells while their expression levels are very low in many epithelial cells [29]. Thus, RGD modified gold nanoparticles should be selectively uptaken by cancer cells. The NLS modification further targets AuNPs to nucleus [30-33]. This dual functionality increases the likelihood of delivery and accumulation of the RGD/NLS modified AuNPs to the nucleus. The accumulation of AuNPs leads to clustering that happens naturally in vitro because AuNPs are coated with RGD peptides which interact with the integrin receptors located on the cellular membrane. NLS peptide (positively charged) coated AuNPs may also be internalized by electrostatic interaction based adsorptive endocytosis. These two mechanisms may lead to clustering of peptide modified AuNPs in the cytoplasm, particularly around the nucleus. The effects of clustering and its relation to energy deposition and nanoparticles size were recently simulated by Monte-Carlo study. It was shown that clustering increased the energy deposited locally [34]. Since we have shown that accumulation of AuNPs in the vicinity of nuclei, the radiation enhancement observed here may be related to the clustering of NLS coated AuNPs that increases the local energy deposited closer to nuclei.

We exploited the strategy combining RGD and NLS peptides targeting cancer cells and nuclei respectively. We showed that the NLS/RGD/PEG modified AuNPs accumulated inside and nearby nucleus (Fig. 2 and 3). It is generally considered that nuclear membrane of cancer cells is defective and accordingly allows passage of larger nanoparticles [31-34]. In this work, the nuclear membrane of A549 cancer cells allowed passage of 40 nm sized gold nanoparticles. Combining increased amount of nuclear-targeted gold nanoparticles and intensified irradiation doses led to reduced cell proliferation and increased cell killing. The radiation enhancement factor was tuned from 1.20 to 1.55 by increased amount of the modified AuNPs. The LQ parameters, α and β, increased in a manner consistent with a dose-modifying effect, suggesting that radiosensitization is mediated primarily by a local increase in dose deposition. Additionally, the increase in alpha suggested a modest LET effect. This outcome suggests that the NLS / RGD modification strategy is valid to make AuNP as a potent radiosensitizer targeting the nucleus, enhancing radiation-induced cell death. This is a successful demonstration that effective cancer cell death was induced by nuclear targeting of AuNPs and X-ray irradiation.

There are many reports that radiation enhancement was varied with parameters such as energy, amount and size of gold nanoparticles, and cell types. The amount of AuNPs in these studies varied greatly from μM to mM. In addition, beam energy was varied from kilovoltage to megavoltage. Particle size was varied from 1.9 nm to 74 nm. Several studies utilized a commercial AuNP with size of 1.9 nm and coated with a proprietary thiol group, but the resulted radiation effect was small [36-44]. One particular study reported by Chithrani et al. showed that radiosensitization was dependent on the number of gold nanoparticles internalized, the size of nanoparticle and the energy used [32]. Gold nanoparticles with diameter of 50 nm were the most effective radiosensitizer but a modest effect on DNA damage was observed. This modest damage may be a result of endosomal entrapment of gold nanoparticles. It is very difficult to make a meaningful comparison because experimental conditions were not comparable with each other. In contrast, there are several reports demonstrating effective cell death achieved by photothermal therapy using nuclear targeted AuNPs [45-47]. Auger-emitting radiopharmaceuticals targeted to the nucleus have also shown efficacy in vitro [48].

Typical irradiation dose at 2 Gy per session is not making a significant effect on the cell survival. This level of irradiation is not sufficient when sub-nanogram or nanogram level of gold nanoparticle is deposited to initiate cell killing. However, successive irradiations at 2 Gy per session would initiate cell killing because we observed that at 4 or 8 Gy per session the cell survival was significantly lowered, suggesting that multisession irradiation (successive irradiation at 2 Gy per session) and nanogram level of gold nanoparticle deposition could be useful. If one succeeds to deposit gold nanoparticles about 10 nanograms at cancer tissues, 2 Gy per session irradiation could be a therapeutic dose.

The peptide modification and stability of the nuclear-targeted AuNPs are highly critical. The positively charged amino acid sequence in the NLS peptide may induce instability during and after peptide modification. We found that the bicarbonate buffer stabilized peptide modified AuNPs for several months. Colloidal instability can be easily observable by agglomeration and precipitation of gold nanoparticles during modification processes. Thus, the stability of peptide modification is a key factor for success of nuclear targeted AuNPs.

5. Conclusion

We exploited RGD and NLS peptides targeting cancer cells and nuclei to initiate radiation-induced cell death. Effectiveness of the nuclear-targeted gold nanoparticles as radiosensitizer was evaluated using A549 cell lines. Increased amount of the nuclear-targeted gold nanoparticles caused radiation enhancement, so lowered irradiation doses would be used for the radiation therapy. This study successfully demonstrates that the nuclear-targeted gold nanoparticles inhibit cellular proliferation and induce cell death. This finding suggests that the NLS / RGD peptide modification is a working strategy to enable AuNP as a potent radiosensitizer for the radiation therapy. We conclude that the NLS/RGD/PEG-AuNP is a good radiotherapeutic candidate and that detailed in vitro experiments with other cell types and in vivo studies should be conducted to better understand sensitization mechanisms.

Acknowledgements

SO thanks to Fulbright Commission for a scholarship partly supporting this work and Melek Özkan Üçüncü, Özge Tüncel, Seçil Sevim Ünlütürk, Justin Klein, and Symantak Khan for their support.

References

[1] Arnold H, 2009 Basic Clinical Radiobiology, Ed. by M. Joiner, 4th Ed., CRC Books p. 1-10

[2] Thariat J, Hannoun-Levi J M, Sun Myint A, Vuong T, Gerard J P 2013 Past, present, and future of radiotherapy for the benefit of patients *Nat. Rev. Clin. Oncol.* **10** 52-60

[3] Hainfeld J F, Slatkin, D Smilowitz H M The use of gold nanoparticles to enhance radiotherapy in mice 2004 *Phys. Med. Biol.* **49** 309-315

[4] Her S, Jaffray D A, Allen C Gold nanoparticles for applications in cancer radiotherapy: Mechanisms and recent advancements 2017 *Adv. Drug Del. Rev*. **109** 84 -101

[5] Cui L, Her S, Borst G R, Bristow R G, Jaffray D A, Allen C. Radiosensitization by gold nanoparticles: will they ever make it to the clinic? 2017 *Radiotherapy and Oncology* **124** 344 – 356

[6] Wang C, Li X, Wang Y, Liu Z, Fu L, Hu L Enhancement of radiation effect and increase of apoptosis in lung cancer cells by thiol-glucose-bound gold nanoparticles at megavoltage radiation energies 2013 *J. Nanoparticle Res.* **15** 1642

[7] Krishnan S, Aliru M 2018 Nuclear-targeted gold nanoparticles as radiosensitizers *Proceedings of the American Association for Cancer Research Annual Meeting*; Chicago, IL. Philadelphia AACR Cancer Res 78-13 Abstract nr 3212

[8] Fertil B, Malaise E P. Intrinsic radiosensitivity of human cell lines is correlated with radioresponsiveness of human tumors analysis of 101 published survival curves 1985 *Int. Radiat. Oncol. Biol. Phys.* **11** 1699 – 1707

[9] Carter J D, Cheng N N, Qu Y, Suarez G D, Guo T Nanoscale energy deposition by X-ray absorbing nanostructures 2007 *J. Phys. Chem. B.* **111** 11622 – 11625

[10] McMahon S J, Hyland W B, Muir M F, Jain S, Butterworth K T et al. Biological consequences of nanoscale energy deposition near irradiated heavy atom nanoparticles 2011 *Sci Rep.* **1** 18

[11] McQuaid H N, Muir M F, Taggart L E, McMahon S J, Coulter J A, Hyland W B et al. Imaging and radiation effects of gold nanoparticles in tumor cells 2015 *Sci. Rep.* **6** 19442

[12] Lechtman E and Pignol J-P Interplay between the gold nanoparticle sub-cellular localization, size, and the photon energy for radiosensitization 2017 *Sci. Rep.* **7** 13268

[13] Hildenbrand G, Metzler P, Pilarczyk G, Bobu V, Kriz W, Hosser H, et al. Dose enhancement effects of gold nanoparticles specifically targeting RNA in breast cancer cells 2018 *PLoS ONE* **13** e0190183

[14] Choi J, Jung KO, Graves E E, Pratx G A gold nanoparticle system for enhancement of radiotherapy and simultaneous monitoring of reactive-oxygen-species formation 2018 *Nanotechnology* **29 50** pp. 504001

[15] Ku A, Facca V J, Cai Z, Reilly R M Auger electrons for cancer therapy – a review 2019 EJNMMI Radiopharmacy and Chemistry **4** 27

[16] McNamara A L, Kam W W Y, Scales N, McMahon S J, J W Bennett J W et al. Dose enhancement effects to the nucleus and mitochondria from gold nanoparticles in the cytosol 2016 *Phys. Med. Biol.* **61** 5993

[17] Tammam S M, Azzazy H M E, Lamprecht A. How successful is nuclear targeting by nanocarriers 2016 *J. Control. Release* **229**, 140 -153

[18] Cai K, Wang A Z, Yin L, Cheng J. 2017 Bio-nano interface: The impact of biological environment on nanomaterials and their delivery properties. *J. Control. Release* **263**, 211-222

[19] Pollard T D, Earshaw W C 2002 *Cell Biology*, Saunders: New York

[20] Petros R A, DeSimone J M Strategies in the design of nanoparticles for therapeutic applications 2010 *Nat. Rev. Drug Discov.* **9**, 615 – 627

[21] Bareford L M, Swaan P W Endocytic mechanisms for targeted drug delivery 2010 Adv. Drug Deliv. Rev. 59 748 – 758

[22] Pelkmans L, Helenius A Endocytosis via caveolae 2002 *Traffic* **3** 311–320

[23] Zink D, Fischer a H, Nickerson J A Nuclear structure in cancer cells, Nat. Rev. Cancer 4 (2004) 677–687

[24] Pouton C W, Wagstaff K M, Roth D M, Moseley G W, Jans D A Targeted delivery to the nucleus, Adv. Drug Deliv. Rev. 59 (2007) 698–717

[25] Panté N, Kann M Nuclear pore complex is able to transport macromolecules with diameters of ~39 nm, 2002 Mol. Biol. Cell 13 425–434

[26] Xu C, Xie J, Kohler N, Walsh E G , Chin Y E, Sun S Monodisperse magnetite nanoparticles coupled with nuclear localization signal peptide for cell-nucleus targeting 2008 Chem. Asian. J. 3 548–552

[27] J.D. Larsen J D , Ross N L, Sullivan M O Requirements for the nuclear entry of polyplexes and nanoparticles during mitosis, J. Gene Med. 14 (2012) 580–589

[28] Guzman C, Bagga M, Kaur A, Westermarck J, Abankwa D ColonyArea: An ImageJ plugin to automatically quantify colony formation in clonogenic assays 2014 *PLoS ONE* **9**, e92444

[29] Kren A, Baeriswyl V, Lehembre F, Wunderlin C, Strittmatter K, Antoniadis H et al. Increased tumor cell dissemination and cellular senescence in the absence of beta-1integrin function 2007 *EMBO J* **26** 2832-2842

[30] Tkachenko A G, Xie H, Coleman D, Glomm W, Ryan J, Anderson M F et al. Multifunctional gold nanoparticle-peptide complexes for nuclear targeting 2003 *J. Am. Chem. Soc.* **125** 4700 – 4701

[31] Kuusisto H V, Wagstaff K M, Alvisi G, Roth D M, Jans D A Global enhancement of nuclear localization dependent nuclear transport in transformed cells. 2012 *FASEB J.* **26** 1181-93

[32] Feldherr C M and Akin D. The permeability of the nuclear envelope in dividing and non-dividing cells cultures 1990 *J. Cell. Biol.* **111** 1-8

[33] Feldherr C M and Akin D Regulation of nuclear transport in proliferating and quiescent cells 1993 *Exp. Cell Res.* **205** 179 – 86

[34] Zutte Villate J M, Hahn M B Radioactive gold nanoparticles for cancer treatment: Size and cluster dependent damage studied by Geant4 Monte-Carlo simulations 2019 Eur. Phys. J. D **73:** 95

[35] Butterworth K T, Coulter J A, Jain S, Forker J, McMahon S J, Schettino G et al. Evaluation of cytotoxicity and radiation enhancement using 1.9 nm gold nanoparticles: potential applications for cancer therapy 2010 *Nanotechnology* **21** 295101

[36] Coulter J A, Jain S, Butterworth K T, Taggart L E, Dickson, G R, McMahon S J et al. Cell type-dependent uptake, localization, and cytotoxicity of 1.9 nm gold nanoparticles 2012 *Int. J. Nanomedicine* **7** 2673 – 2685

[37] Cui L, Tse K, Zahedi P, Harding S M, Zafarana G, Jaffray D A et al. Hypoxia and cellular localization influence the radiosensitizing effect of gold nanoparticles in breast cancer cells 2014 *Radiat. Res.* **182** 475 – 488

[38] Jain S, Coulter J A, Butterworth K T, Hounsell A R, McMahon S J, Hyland W B et al. Gold nanoparticle cellular uptake, toxicity, and radiosensitization in hypoxic conditions 2014 *Radither. Oncol* **110** 342 – 347

[39] Jain S, Coulter J A, Hounsell A R, Butterworth K T, McMahon S J, Hyland W B et al. Cell specific radiosensitization by gold nanoparticles at megavoltage radiation energies 2011 *Int. J. Radiat. Oncol. Biol. Phys.* 531 – 539

[40] Lui C-J, Wang C-H, Chien C-C, Yang T-Y, Chen S-T, Leng W-H et al. Enhanced X-ray irradiation induced cancer cell damage by gold nanoparticles treated by a new synthesis method of polyethylene glycol modification 2008 *Nanotechnology* **19** 295104

[41] Rahman W N, Bishara N, Ackerly T, He C F, Jackson P, Wong C et al. Enhancement of radiation effects by gold nanoparticles for superficial radiation therapy 2009 *Nanomed Nanotechnol. Biol. Med.* **5** 136 – 142

[42] Taggart L E, McMahon S J, Currell F J, Prise K M, Butterworth K T The role of mitochondrial function in gold nanoparticle mediated radiosensitization 2014 Cancer Nanotechnol. **5** 5

[43] Zhang X-D, Chen J, Luo Z, Wu D, Shen X, Song S-S et al. Enhanced tumor accumulation of sub-2nm gold nanoclusters for cancer radiation therapy 2014 *Adv. Healthcare Mater.* **3** 133 -141

[44] Chithrani D B, Jelveh S, Jalali F, van Proojien M, Allen C, Bristow R G et al. Gold nanoparticles as radiation sensitizers in cancer therapy 2010 *Radiation Res.* **173** 719 – 728

[45] Hirsch L R, Stafford R J, Bankson J A, Sershen S R, Rivera B, Price R E et al. Nanoscale mediated near infrared thermal therapy of tumors under magnetic resonance guidance 2003 *Proc. Natl. Acad. Sci. U.S.A.* **100** 13549 – 13554

[46] Kennedy L C, Bickford L R, Lewinski N A, Coughlin A J, Day E S, West J L et al. 2011 A new era for cancer treatment: gold nanoparticle mediated thermal therapies *Small* **7** 169 – 183

[47] Hainfeld J F, Lin L, Slatkin D N, Dilmanian F A, Vadas T M, Smilowitz H M Gold nanoparticles hyperthermia reduces radiotherapy doses 2014 *Nanomed. Nanotechnol. Bio. Med.* **10** 1609 – 1617

[48] Constantini D L, Chan C, Cai Z., Vallis K A, Reilly R M ^{111}In-Labeled Trastuzumab (Herceptin) Modified with Nuclear Localization Sequences (NLS): An Auger Electron-Emitting Radiotherapeutic Agent for HER2/neu-Amplified Breast Cancer 2007 J.Nucl.Med. **48**, 1357-1368